

Structural control on badland slope evolution: A case study from the southern Apennines (Italy)

M. Bentivenga ^{a,*}, F. Agosta ^{a,b}, G. Palladino ^c, M. Piccarreta ^d, G. Prosser ^a

^a Dipartimento di Scienze, University of Basilicata, I-85100 Potenza, Italy

^b Geosmart Italia, Italy

^c Department of Geology and Geophysics, School of Geosciences, University of Aberdeen, Aberdeen, UK

^d Ministero della Pubblica Istruzione, Italy

ARTICLE INFO

Article history:

Received 16 January 2020

Received in revised form 12 November 2020

Accepted 13 November 2020

Available online 17 November 2020

Keywords:

Badland evolution

Riedel fractures

Clay deformation

Fault zones

Southern Italy

ABSTRACT

This work focuses on a multi-method study of badlands exposed in two different areas of southern Italy. Results of both geomorphological and structural geological studies are obtained by combining field and laboratory analyses of the badlands affecting Plio-Quaternary silty-clays of southern Italy. Results are discussed in terms of deformation mechanisms and badland formation and evolution. Results highlight the role played by pre-existing structural heterogeneities, such as high-angle faults and joints, on both gravitational processes and water circulation. The aforementioned heterogeneities are due to specific tectonic stress regimes, and are interpreted in light of their genetic nature, kinematics, attitude, geometry, relative timing of formation, and aerial distribution. Results of this work are summarized in a four-stage conceptual model characterized by specific genetic mechanisms. The conceptual model includes representative sketches aimed at assessing the time-dependant evolution of the badlands. A profound link between structural geology and geomorphological processes is therefore envisioned for the badlands of southern Italy.

© 2020 Elsevier B.V. All rights reserved.

1. Introduction

Badlands derive from fast-linear erosion that develops in clay-rich lithologies. They generally consist of ca. 40° to 50° steep cliffs, which are deeply incised by rills separated from each other by ridges showing a “knife-edge” geometry. Their formation and development are mainly controlled by climate, tectonics, and landuse changes (Joshi and Nagare, 2013; Castaldi and Chiochini, 2012; Moretti and Rodolfi, 2000; Torri et al., 1994). In fact, badlands are commonly present in areas subjected to tectonic uplift, and characterized by high average annual temperatures, and both scarce and unevenly distributed precipitations (Mather et al., 2002; Del Prete et al., 1994, 1997; Moreno de las Heras and Gallart, 2018; Piccarreta et al., 2006; Vergari et al., 2011). These erosional features derive from the effects of water washout on degraded clays along steep, south-facing clay rich slopes in areas characterized by a high drainage density and a scarce vegetation cover. Commonly, badland landforms are subdivided into two predominant morphologies (Fig. 1), represented by the main badland slope, and by residual dome-shaped forms located at the base of the badland slopes, known locally as “Biancane” (Alexander, 1982; Colica and Guasparri, 1990; Torri and Bryan, 1997; Torri et al., 1994; Calzolari and Ungaro, 1998; Del Prete et al., 1994).

The control exerted by tectonic discontinuities on badlands formation has been studied by several authors (Colica and Guasparri, 1990; Farifteh and Soeters, 2006; Calzolari and Ungaro, 1998; Joshi and Nagare, 2013), who assessed the influence of large-scale structural heterogeneities of rock mass, mainly detected from aerial and satellite imagery, on weathering, erosion and drainage development in badlands. However, field analyses of the relationships between badland morphology and the occurrence of fractures and faults within claystones have not been performed so far. In order to fill this gap, in the present work a detailed structural analysis has been carried out in order to decipher how tectonic discontinuities influence the morphology and the evolution of the badland slopes, in combination with gravity-induced phenomena. In addition, processes responsible for the formation of conduits that allow water circulation in clays, favoring the development of badland morphologies, will be investigated. The study has been carried out by analyzing badland formation in two representative areas of the Basilicata Region, Italy, where they cover an area of approximately 3000 km². In these areas, we focus on the origin of dome-shaped forms (Fig. 1) and on the overall evolution of the badland slopes.

The two studied areas are located along the hinterland domain of the Ionian coastline (Fig. 2), in which Plio-Pleistocene claystones widely crop out (Bentivenga et al., 2004a, 2004b, 2015; Bentivenga and Piccarreta, 2016). In the past, these claystones were investigated to unravel the genetic mechanisms of badlands focusing on the role played by climate (Vittorini, 1977; Alexander, 1982; Dramis et al., 1982; Del Prete et al., 1994, 1997; Del Monte, 2017; Neugirg et al., 2016), grain size and

* Corresponding author.

E-mail addresses: mario.bentivenga@unibas.it (M. Bentivenga),

[URL: https://www.geosmartitalia.it](http://www.geosmartitalia.it) (F. Agosta).

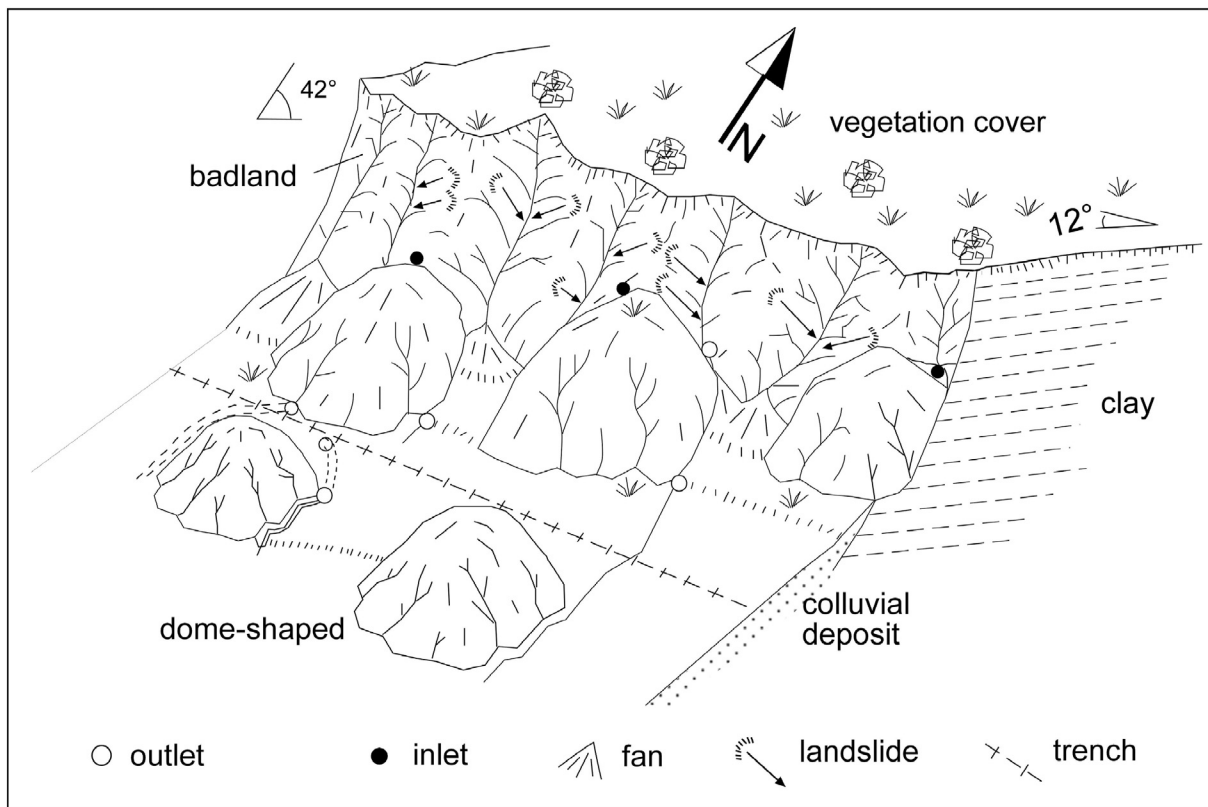


Fig. 1. Scheme of the badland slopes and associated dome-shaped forms (Piccarreta et al., 2006).

mineralogy (Alexander, 1982; Del Prete et al., 1994; Farifteh and Soeters, 1999; Battaglia et al., 2002; Piccarreta et al., 2006; Summa et al., 2007).

The two chosen areas are fully representative of most of the badland morphologies found in other areas of Italy and many occurrences

worldwide. Furthermore, the choice of the studied sites was also dictated by the different chemical and physical characteristics of the outcropping clays, affected by the different badland forms (Piccarreta et al., 2006; Vergari et al., 2013). At these sites we take advantage of

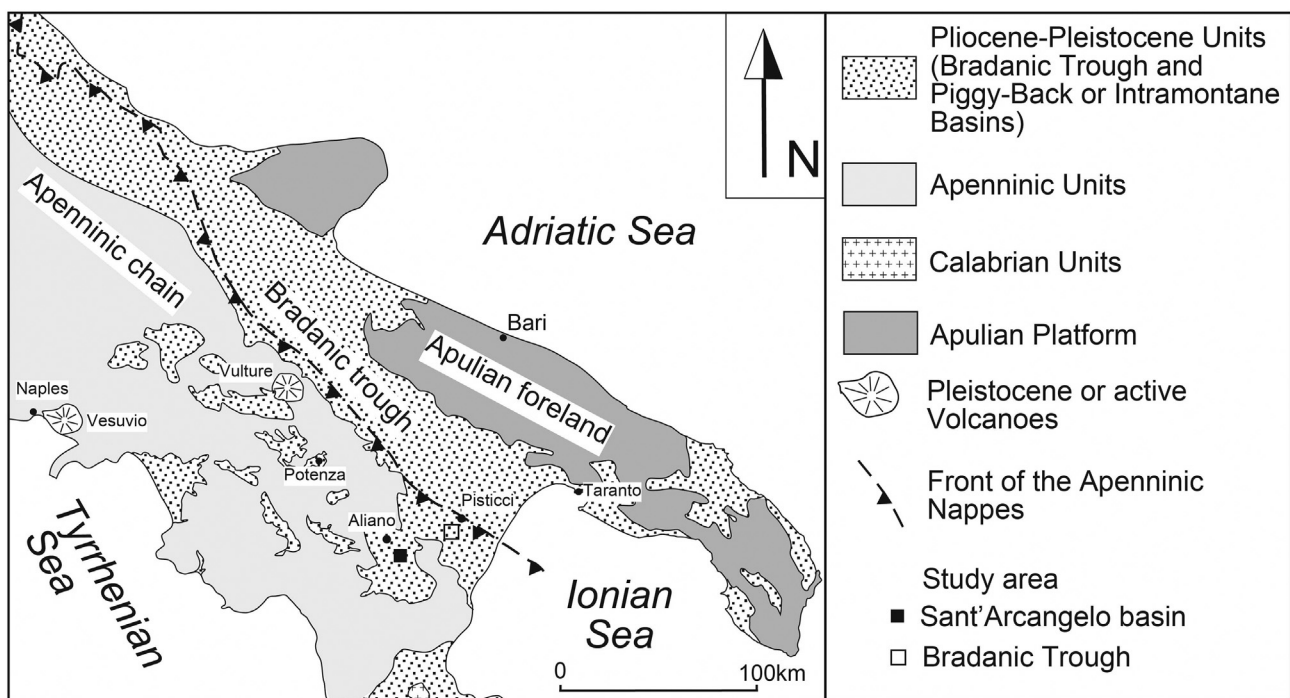


Fig. 2. Geological sketch map of the southern Apennines. Location of the two study areas of the Sant'Arcangelo Basin and Bradanic Trough is reported (modified after Bentivenga et al., 2004a, 2004b).

the numerous fractures and faults that crosscut the claystones to focus on the both formation and growth of badland slopes and dome-shaped forms. Results of combined structural and geomorphological studies are summarized into a conceptual model of fracture- and fault-controlled badland formation.

2. Geological setting

The two study areas, representing good examples on the role exerted by tectonic structures in the development of badland slopes, are located in the vicinity of the Aliano and Pisticci towns, respectively. The former one is exposed at altitudes comprised between 50 and 150 m a.s.l., the other one at altitudes in between 350 and 650 m a.s.l., respectively. The Aliano area lies along the northern sector of the Sant'Arcangelo Basin, whereas the Pisticci area is positioned along the south-western portion of the Bradano Trough. Both the Sant'Arcangelo Basin and Bradano Trough are part of the outer domains of the southern Apennines fold-and-thrust belt (Fig. 2), a Cenozoic circum-Mediterranean orogeny developed due

to Eurasian and African plate convergence (Mantovani et al., 1996; Patacca and Scandone, 2007).

The southern Apennines fold-and-thrust belt consists of a stack of tectonic units derived from the Adria passive margin and the Ligurian Ocean (D'Argenio et al., 1973; D'Argenio and Alvarez, 1980). These tectonic units form a multi-duplex as a result of both thin-skinned (Roure et al., 1991; Monaco et al., 1998; Menardi Noguera and Rea, 2000) and thick-skinned tectonics (Shiner et al., 2004; Mazzoli et al., 2006; La Bruna et al., 2017, 2018). Contractive tectonics was accompanied by formation of Early Miocene-Pleistocene thrust-top basins and foredeep basins at the top of single thrust sheets and at belt front, respectively (Hippolyte et al., 1994; Pieri et al., 1997; Vezzani et al., 2010; Palladino, 2011). During Pleistocene the whole belt underwent to transtensional faulting (Westaway, 1993; Patacca and Scandone, 2001; Bavusi et al., 2004; Giano et al., 2018), whose activity migrated eastwards due to opening of the Tyrrhenian Sea (Royden et al., 1987; Doglioni, 1991), gravitational collapse of the belt (Ghissetti and Vezzani, 1999; Ghissetti et al., 2001), and/or interaction with the Calabrian Arc (Turco et al., 1990).

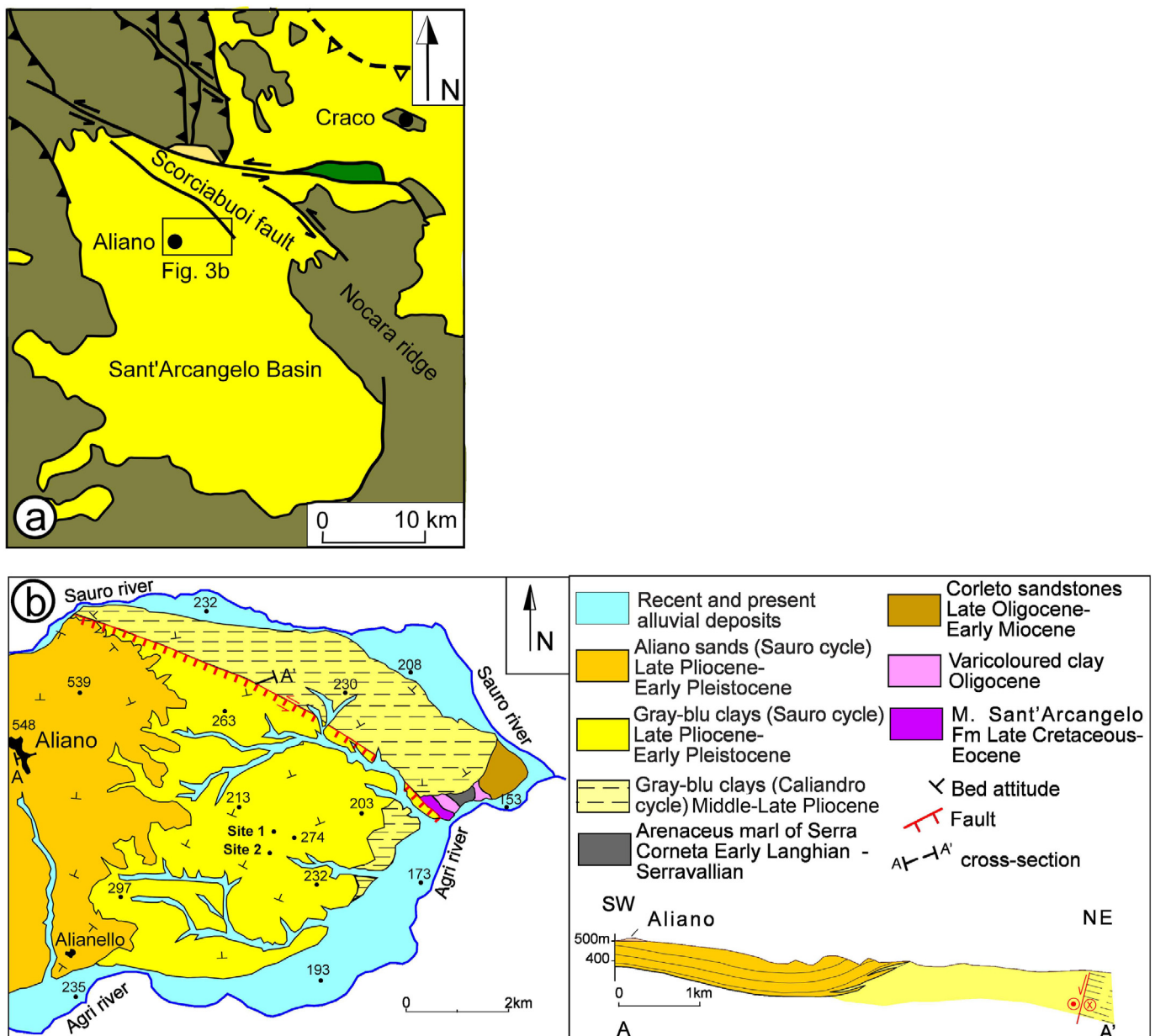


Fig. 3. a) Tectonic sketch map of the Sant'Arcangelo Basin, modified after Bentivenga et al. (2005); b) Geological map of Aliano area (modified after Pieri et al., 1994).

2.1. Sant'Arcangelo Basin

The Sant'Arcangelo Basin consists of a Plio-Pleistocene thrust-top basin (Caldara et al., 1988; Hippolyte et al., 1991), characterized by a 40 km-long, 18 km-wide, NW-SE elongated shape filled with up to 5 km-thick Plio-Quaternary clastic sediments (Pieri et al., 1994; Patacca and Scandone, 2001). Two main sedimentary sequences are present (Vezzani, 1967; Ogniben, 1969; Lentini and Vezzani, 1974; Zavala and Mutti, 1996). The first one, Late Pliocene in age, consists of an up to 1.4 km-thick, syn-tectonic transgressive-regressive fan delta sequence. The second one, Late Pliocene-Calabrian in age, consists of up to 0.9 km-thick conglomerates, sands, and marly clays unconformably topped by Middle Pleistocene alluvial to lacustrine continental deposits (Sabato, 1997). The Aliano area (Fig. 3) exposes mainly marly clays of Calabrian age, containing some meter's thick intercalations of sandstone beds. These lithologies have been affected by tectonic uplift, folding and the activity of WNW-ESE-striking traseensional faults during the Pleistocene evolution of the Sant'Arcangelo basin (Catalano et al., 1993; Casciello et al., 2000; Casciello, 2002; Caputo et al., 2007; Giano and Giannandrea, 2014).

2.2. Bradano Trough

The Bradano Trough is part of the southern Apennines foredeep filled with up to 2 km-thick Plio-Pleistocene sediments (Migliorini, 1937; Selli, 1962; Casnedi, 1988; Pieri et al., 1996; Monaco et al., 1998; Calamita et al., 1999). The transgressive-regressive sedimentary infill progressively thins towards the NE, and includes clayey marls, turbiditic sandstones and clays, shelfal mudstones, and shallow-water sands and conglomerates (Balduzzi et al., 1982; Patacca and Scandone, 2001). The Pisticci area exposes the Lower Pleistocene sedimentary sequence, which consists of marly clays and clayey marls (Fig. 4). Locally, carbonate concretions and lenticular-shaped sand/silt deposits and volcanic ashes are present. The clayey deposits are very well compacted and are often crosscut by conchoidal fractures. The studied area was affected by a moderate deformation, due to coeval normal faulting of the Ionian coastline and tectonic uplift of the frontal portions of the belt (Pieri et al., 1997; Bentivenga et al., 2004a, 2004b).

3. Geomorphological setting

The southern Apennines mountain belt reaches an elevation up to ca. 2 km a.s.l., and is characterized by an approximately NW-SE oriented

watershed separating drainage systems directed towards the surrounding marine basins. From a geomorphological perspective, the southern Apennines can be divided into three separated domains referred to as internal, axial and external, from west to east, respectively. The internal domain corresponds to the Tyrrhenian side of the chain, the axial one identifies the tallest portion of the belt, which corresponds to the remnants of Pliocene to Pleistocene erosional land surfaces that were uplifted and dismembered by Quaternary faults (Schiattarella et al., 2013). The external domain includes Plio-Quaternary thrust-top and foredeep basins, and it is characterized by a predominant hilly landscape incised by river valleys-oriented ca. E-W, in the north, and NW-SE, in the south.

The Sant'Arcangelo Basin is located in the outer domain of the Southern Apennines, in the vicinity of the Ionian Sea. This basin is landlocked by the mountain belt, and bounded by the large-scale Scorciabuoi Fault, to the north (Fig. 3a). Its clastic infill is crosscut by the Agri and Sinni rivers, which formed widespread alluvial terraces (Cinque et al., 1993). An uplift rate comprised between 0.7 and 0.9 mm/year has been estimated (Schiattarella et al., 2006; Giano and Giannandrea, 2014). The Bradanic Trough extends from the Adriatic Sea to the Gulf of Taranto, and lies in the outer domain of the Southern Apennines as well. Starting from the Middle Pleistocene, it was gradually uplifted together with the progressive migration of the coast line. This regressive stage led to the deposition of sands and conglomerates, and formation of different terraced surfaces in some cases disrupted by high-angle normal faults (Bentivenga et al., 2004a, 2004b; Amato, 2000; Cotecchia and Magri, 1967; Neboit, 1982; Westaway, 1993; Westaway and Bridgland, 2007; Hearnthy and Dai Pra, 1992). Tectonic processes during uplift were responsible for a general dip towards the NE of the Pleistocene deposits. According to the inferred ages of the marine terraces, the average uplift rate is comprised between 0.2 and 1.0 mm/year (Neboit, 1982; Westaway, 1993; Amato, 2000; Bentivenga et al., 2004a, 2004b).

In the studied areas, erosion of the terraced surfaces by the development of a hydrographic network generated isolated flat areas, which are today surrounded by steep slopes exposing Plio-Pleistocene clays, and Pleistocene sands/conglomerates. The steep slopes are very unstable, and frequently affected by landslides and/or badlands morphologies. As a common rule, badlands have formed from the incision of tension cracks formed in the landslide source area (Vergari et al., 2019). Morphologically, the upper portions of the slopes are generally characterized by landslides and badlands, whereas the lower portions by badland slopes and dome-shaped forms (Mather et al., 2002; Piccarreta et al., 2006; Bentivenga and Piccarreta, 2016; Moreno de las Heras and Gallart, 2018).

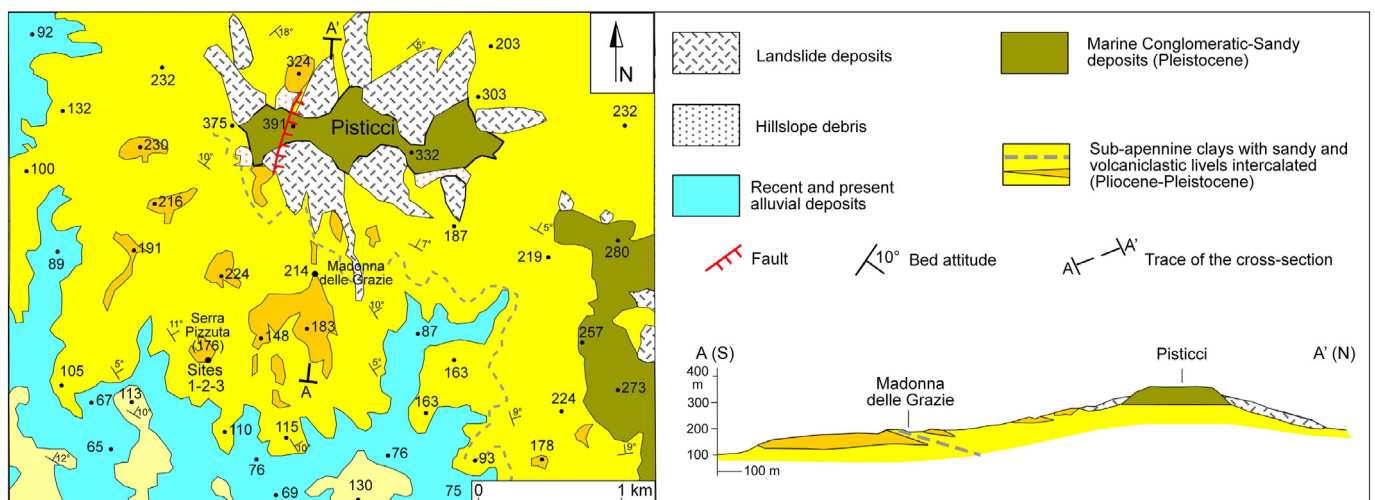


Fig. 4. Geological map of the Pisticci area.

4. Materials and methods

The present study focuses on two selected sites located in the Aliano area (Site #1 - 202 m a.s.l. - $40^{\circ}18'02.17''\text{N}$ - $16^{\circ}17'22.17''\text{E}$; Site #2 - 274 m a.s.l. - $40^{\circ}18'03.70''\text{N}$ - $16^{\circ}17'23.61''\text{E}$), and on one site, named as Serra Pizzuta, in the Pisticci area (Site #3 - 274 m a.s.l. - $40^{\circ}22'21.20''\text{N}$ - $16^{\circ}32'38.57''\text{E}$). There, the badlands have developed into north- to northeast-dipping Plio-Pleistocene clays arranged into monoclinals with steep southern slopes (Pieri et al., 1994; Pieri et al., 1997; Bentivenga et al., 2004a, 2004b). The three sites were selected after a careful geomorphological mapping of the studied areas (Bentivenga and Piccarreta, 2016). The study sites are all located in the lowermost portion of the slopes (Piccarreta et al., 2006), where the badland slopes and associated dome-shaped forms of variable shapes and sizes are clearly exposed, and representative of other badlands occurring elsewhere in Italy (Vittorini, 1977; Sdao et al., 1984; Vergari et al., 2013) and Spain (Mather et al., 2002; Joshi and Nagare, 2013).

The geological study was performed by means of integrated stereoscopic analysis of recent aerial photos (1:33.000 scale), and both structural and geomorphological field investigations. Stereoscopic analysis allowed us to identify and then select the sites for subsequent detailed field surveys. Geomorphological field analysis was carried out by mapping the badland morphologies present along the south-facing slopes of the monoclinal systems, and the landslides and small tension cracks that affect the north-facing slopes. In Site #3 located in the Pisticci area, observations were carried out along three measurement transect oriented orthogonal to the E-W trending badland slope.

This work was then integrated with Unmanned Aerial Vehicle (UAV) image acquisition, and subsequent 3D modelling of the areas by using the Agisoft Metashape software, which permitted the digital image analysis of the studied sites.

Field structural analysis was carried out by measuring discontinuities with a geological compass on key outcrops exposing transects including the badland slopes and the dome-shaped forms. Fractures in marly clay have been classified on the basis of the measured orientations and the observed geometrical relationships. In some cases, in order to understand the meaning and evolution of fractures, measured orientations have been rotated by restoring the bedding attitude to the horizontal. Outcrops were investigated after the removal of about 10 cm-thick portions of weathered dry clay. Such a procedure was necessary to distinguish fractures that crosscut the clay beds from mudcracks, which are localized within the outermost, dried portion of the clay outcrops. Mm-thick, cohesive structural elements were sampled and analysed by optical microscope and digital image analyses. Cm-wide images of the slab obtained from these samples were interpreted in light of a well-known structural models for sheared clayish material (Twiss and Moores, 2007). They include mm- to cm-thick shear zones containing a variety of microfractures showing either synthetic or antithetic geometries with respect to the main slip surfaces.

Furthermore, the results of both geomorphological and structural analyses were compared and discussed in order to assess the possible relationships between fractures and water circulation at shallow levels in badland areas, responsible for the formation of pipes in claystones.

For this purpose, it was carried out a careful characterization of pipe geometries and locations with respect to tectonic discontinuities within the Plio-Pleistocene clay.

5. Results

5.1. Aliano study area, geomorphological analysis

A large badlands area is exposed to the east of Aliano town. The studied area is located in between the middle segment of the Agri River and



Fig. 5. View of the sites in the badlands area of Aliano.

the lowermost portion of the Sauro River (Fig. 3b). There, sandy and clayey deposits display a general dip towards the NE, due to the propagation of contractional structures in the Pleistocene infill of the Sant'Arcangelo Basin (Patacca and Scandone, 2007). As a result, the NE-dipping monoclines are characterized by steep southern slopes, and more shallow-dipping northern slopes. The roughly E-W trending south-facing slopes are characterized by badlands, and by dome-shaped forms located at the base of the steep slopes. The badlands are incised by streams flowing to the east, which are tributaries to the Agri River. The badlands show a herbaceous and shrubby vegetation at their top. This cover is due to the discrete and randomly distributed rainfall (713 mm/y), which characterizes the inner areas of the Basilicata Region, and temperatures comprised year-long between ca. 10 °C (Tmin) and 16.5 °C (Tmax, Piccarreta et al., 2005, 2013, 2015).

The two sites studied at Aliano are shown in Fig. 5. The first one, Site #1, is ca. 40 m-long, 10 m-high, and exposes three different dome-shaped forms. Site #2, is ca. 30 m-long, 12 m-high, and exposes a single dome-shaped form. Site #1 represents a typical case of association between badland slopes and dome-shaped forms. There, the badland slope trends ca. E-W, and shows a slope angle of about 50°. The dip angle of clay-rich beds is ca. 30° N. Both badland slope and dome-shaped forms are characterized by a dense network of rills, due to flow of eroded material that takes place during rare, severe, rainwater precipitation, and by mud cracks forming a complex texture at surface. The geomorphological survey is carried out along the SW margin of the badland slope, in correspondence with a partially detached dome-shaped form, and two other similar forms located adjacent to the slope. Within the transition zone between the badland slope and the dome-shaped forms, rills localize within individual mud cracks (Fig. 6).

At Site #2, the badland slope trends ca. E-W, is mainly exposed southward, and characterized by a slope angle of about 50° (Fig. 7). In the topmost portion of the badland slope, marly clay contain a 1.5 m-thick sand bed, forming a laterally continuous intercalation throughout the entire Site #2. Occurrence of this harder cap rock determines a steeply inclined profile, which becomes less inclined in the lower part of the slope, where the claystones crop out (Fig. 7). The sandy level is affected by various fractures and cavities, which facilitate frequent falls. The study site consists of a badland slope with partially detached and

isolated dome-shaped forms. These forms are elongated orthogonally to the front, up to 2 m-high, and very steep (up to 70–80°). At the top of a dome-shaped form, the sand bed (Fig. 7) is characterized by a steeper dip with respect to the same bed exposed in the badland slope.

5.2. Aliano study area, structural analysis

At Site #1, the badland slopes and associated dome-shaped forms are crosscut by two sets of fractures striking ca. E-W and dipping either ~80°N (Set 1a) or ~40°S (Set 1b). A third set (Set 2) strikes ca. NW-SE, and dips ~85°NE (Fig. 8). Set 1b fractures are the most persistent and long among the whole fracture network exposed in the surveyed outcrops at Site #1. In fact, both Set 1a and Set 2 fractures consist of short, up to ca. 10 cm-high fractures, which are rarely observed along horizontal exposures located at the base of the badland slope. Most of the fractures pertaining to Set 1 and Set 2 abut against Set 1b fractures. Only the largest Set 1a and Set 2 fractures crosscut Set 1b fractures. By restoring the bedding attitude to horizontal, we note that most of the surveyed sets of the 1a and 1b fractures surfaces not only display a normal component of displacement, but also dip ca. 60°N or 60°S. Differently, Set 2 fractures show dip angles of ca. 65–70°NE (Fig. 8). At Site #2, three main sets of fractures are documented. Two fracture sets strike ca. E-W, and dip either 60–70° N (Set 1a) or ca. 30–40°S (Set 1b). The third set (Set 2) strikes ca. NW-SE, and consists of sub-vertical structural elements (Fig. 8). By restoring the bedding attitude to horizontal, the three sets form a structural configuration similar to Site #1, consisting of the two conjugate sets 1a and 1b, dipping 60°N and 60°S, respectively, and Set 2, which dips steeply to the NE (Fig. 8).

5.3. Pisticci study area, geomorphological analysis

The study site (Site #3) is located in the Pisticci area, in correspondence with the Serra Pizzuta locality. It is an E-W trending, 200 m-long, 12 m-high badland area, characterized by a poor vegetation cover due to a mean rainfall of 581 mm/yr concentrated in few severe high magnitude events, and long-lasting drought periods (Piccarreta et al., 2005, 2013, 2015). Observations were conducted along three different measurement transects (Fig. 9). Transect #1, in the westernmost

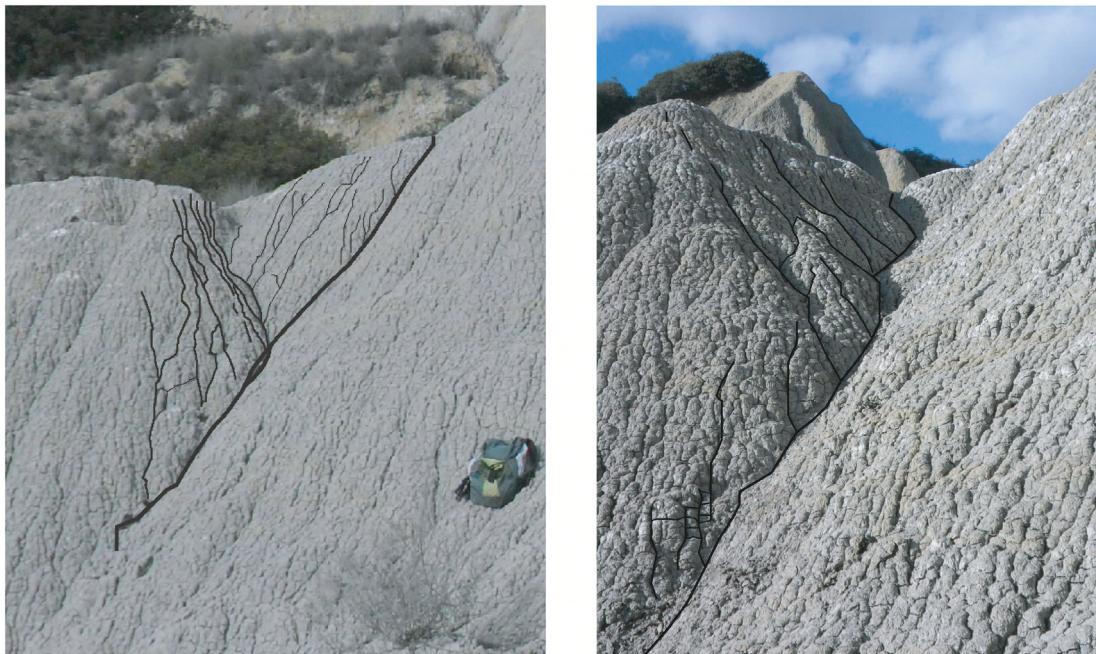


Fig. 6. Outcrop view of the dome-shaped forms exposed at sites #1 and #2. The line drawing highlights the traces of open fractures dissecting the claystones. Three main sets of fractures are depicted, which show a dendritic pattern due to specific abutting relationships. See text for details.



Fig. 7. Badland slope and dome shaped forms with a sandy level at the top.

part of the area, exposes a trench, representing a linear depression located between the badland front and dome shaped forms, infilled with colluvial deposits. The main front, facing south, is characterized by a 45° slope and is marked by deeply incised rills. The claystone beds dip 12° NE. Along the transect, the first dome-shaped form is present ca. 5 m away from the front. It is approximately 12 m-long, 8 m-wide, and 3 m-high, and topped by a 1 m-thick colluvial material (Fig. 10a).

The second transect is located in correspondence of badlands with a slope of about 42° . There, two dome-shaped forms are present ca. 2 m and 8 m away from the slope, respectively (Fig. 10b). The slope is deeply incised by rills forming a “knife-edge” ridge morphology, and separated from the dome-shaped forms by trenches partially filled with colluvial deposits. At the base of the slope, the clay-rich beds are ca. 6° steeper relative to the topmost beds. According to the dip angle of the beds, the dome-shaped form can be subdivided into three sectors (Fig. 11). The first one shows beds dipping 6° to 10° , the second one beds dipping 13° to 18° , the third one beds dipping 6° to 10° . Accordingly, the second sector was affected by rotational, small-sized slides as depicted along transect #2. There, beds dip towards N with small angles at the front, whereas they dip NE with greater angles in correspondence of the dome-shaped forms.

Transect #3 is located along the eastern part of the studied area. There, badlands are also characterized by a slope of approximately 45° , and the large trench at the bottom is flanked by a large dome-shaped form (Fig. 10b). The strike direction of the clay-rich beds is ca. 340° – 360° N, and their dip angle varies upward from ca. 20° to ca. 4° .

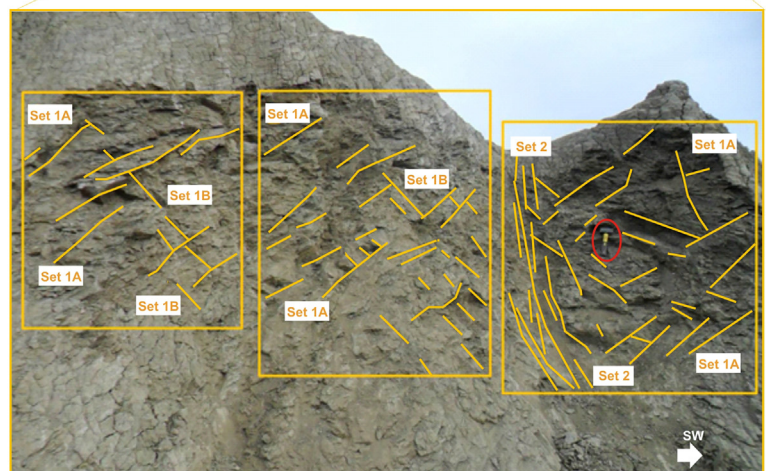
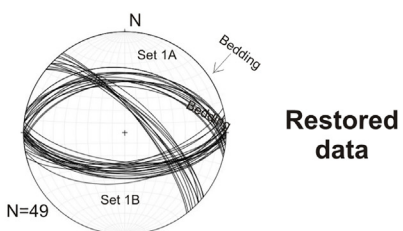
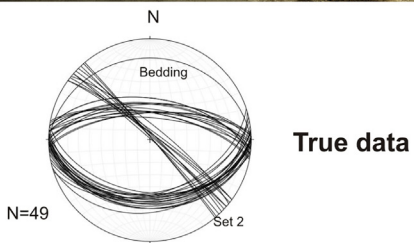
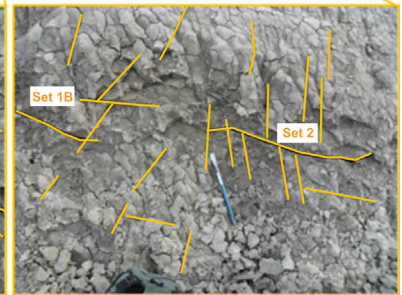
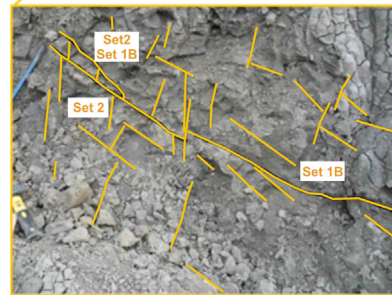
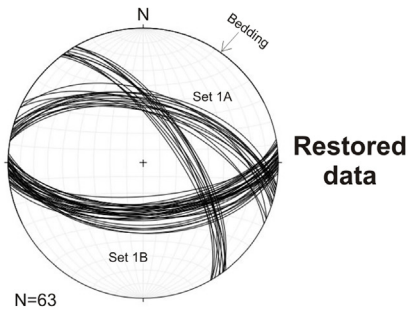
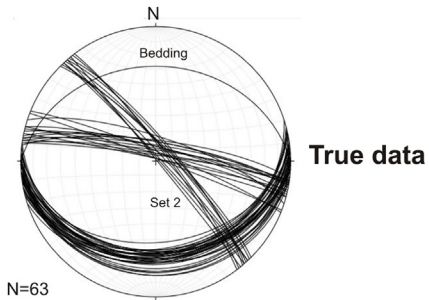
5.4. Pisticci study area, structural analysis

Field structural analyses are performed in N- to NE-dipping clay-rich beds, with angles varying between ca. 5° and 15° (Fig. 11). A northeastward directed tilting of the beds is hence documented within the badland slopes and associated dome-shaped forms (Fig. 12). Along the transects, the fracture networks present at the badland slope and the dome-shaped forms do not show the same geometry and architecture. At the slope portion, two main sets of fractures are present (Fig. 12). By considering the nomenclature used for the Aliano study area, we document Set 2 fractures (ca. NW-SE striking) forming two distinct sets dipping ca. 50° NE (Set 2a) and 50° SW (Set 2b), respectively. Set

3 fractures, not documented at Aliano, consist of N-striking, sub-vertical, sheared fractures displaying strike-slip kinematics forming relay ramps along dip (Fig. 12). Set 3 is made up of mm-thick, left-lateral shear fractures that form the most prominent structural element along the whole surveyed frontal portion of the badlands.

The outcrops located in the dome-shaped forms expose key structural elements and geometries. In fact, Set 1b extensional shear fractures are documented only in the dome-shaped area (Fig. 11). There, Set 1b extensional shear fractures displace a few mm some Set 3 fractures, showing normal components of slip (Fig. 11). Set 3 shear fractures consist of mm-wide, open fractures partially infilled with reddish, uncohesive material. These are well exposed along small pavements, where they form 10's of cm-long segments characterized by enechelon geometries (Fig. 11). These segments are not connected with each other because consist of right-stepping underlapped, left-lateral sheared fractures, separated by contractional jogs. Near the tip of Set 3 shear fractures (mode II termination according to Scholz, 2002), Set 2 fractures are present in the extensional quadrants, forming well-known geometries associated to strike-slip fault growth by means of opening mode (mode I) fractures located within the evolving process zones (Myers and Aydin, 2004). This is well illustrated by the relationship between the ca. N-S (Set 3) and NW-SE (Set 2) fractures, documented near the tip line, at its extensional quadrant, of a left-lateral Set 3 segment (Fig. 11). Set 2 fractures form two distinctive sets (Set 2a and 2b), which dip ca. 50° or ca. 30° either SW or NE, respectively (Fig. 12). Both sets are characterized by mm-thick, vertically persistent elements made up of foliated, not very cohesive clay with a marked darker colour with respect to the parental host rock.

Images of hand specimens collected from key outcrops exposing Set 1b and Set 3 fractures show presence of discontinuities (Fig. 13), whose geometries and attitudes resemble those predicted for the Riedel fractures (Twiss and Moores, 2007). By considering an image of the slab orthogonal to the E-W striking, S-dipping, Set1b fracture cropping out along transect 3 in the dome-shaped forms (Fig. 13), we note that four distinctive fracture sets are recognized (Fig. 13). Y-Riedel shear structures are the most common, and form mm-high, isolated segments that sub-parallel the edges of the sampled structural element. P-Riedel shear structures are also present, and form clusters made up of mm-high fractures synthetic with respect to the Y-Riedel shear structures. Antithetic R'-Riedel and X- Riedel shear structures are also present



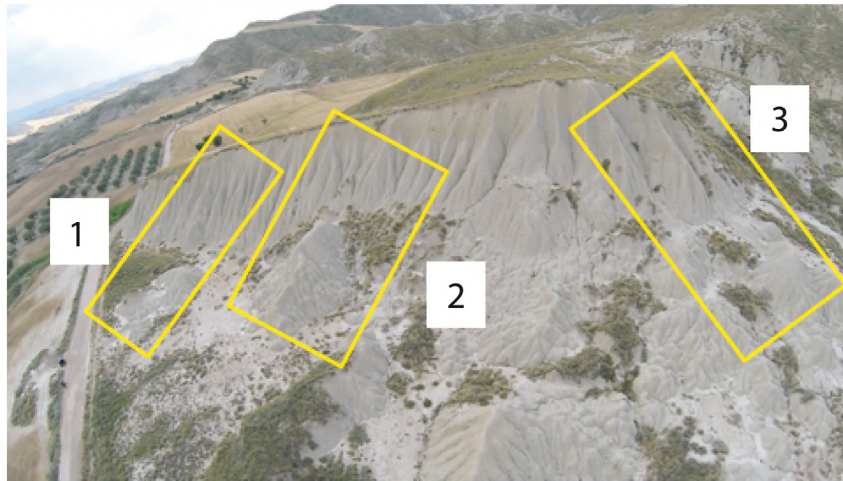


Fig. 9. Badlands area of Serra Pizzuta of Pisticci, with indication of the three measurement transects.

within two small portions of the study image, forming up to a few mm-long features that crosscut the whole, cm-thick shear zone characterized by normal components of slip. The second sample derived from a Set 3 fracture, which was sampled near the tip zone of a 10's of cm-long, sheared element. In this case, the Y-Riedel shear structure elements are made up of up to a few mm-long fractures and both synthetic P-Riedel and R-Riedel fractures are present. These two sheared fracture sets are well-developed within the left-lateral, strike-slip shear zone, bounding isolated rock fragments characterized by squared and rectangular shapes (Fig. 13).

6. Discussion

6.1. Aliano study area

Both shear fracture Sets 1a and 1b crosscut the bedding with a ca. 60° cut-off angle. Bedding restoration to horizontal allows an appreciation that the two fracture sets are characterized by normal components of slip, and can be therefore interpreted as forming a conjugate, Andersonian, E-W striking extensional system. The individual shear fracture sets likely formed during shallow burial of the claystones (Vezzani, 1967), prior to bed tilting, due to the consistent extensional geometry of Sets 1a and 1b shear fractures after bedding restoration to horizontal. Coeval formation of the aforementioned conjugate shear fracture system produced a ca. N-S trending, horizontal positive elongation (Twiss and Moores, 2007). Due to their length, amount of displacement, and inner structural architecture, both shear fracture sets were likely passively rotated, and possibly re-sheared, during uplift and exhumation from shallow depths (Agosta and Aydin, 2006). Set 2 fractures post-date both Sets 1a and 1b and show left-lateral strike-slip kinematics. According to both crosscutting relationships and cut-off angles with bedding, Set 2 fractures are interpreted as shear fractures postdating the bed tilting. As for the previous case, left-lateral motion along Set 2 fractures caused a ca. N-S trending, horizontal positive elongation. For this reason, we interpret that Set 1a, Set 1b and Set 2 shear fractures to have formed under a similar stress field configuration, which was characterized by $\sigma_1 - \sigma_2$ stress permutation over time and rock exhumation from depth. Erosion of the sedimentary pile on top of the studied claystones was hence accompanied by gentle bed tilting, and a relative greater magnitude of the compressive tectonic principal stress axis,

oriented ca. E-W (Twiss and Moores, 2007). The orientation of the tectonic principal stress axis is consistent with left-lateral shearing along the N-120° trending Scoriabuoi fault (Fig. 3a) during the Early Pleistocene (Casciello, 2002; Caputo et al., 2007).

From a geomorphological point of view, Set 1b shear fractures favoured the gravitational collapse of the badlands slope. Since they strike almost parallel to it, gravitational mass processes localized along the Set 1B structural elements. These processes caused bed tilting due to the rotational component, which generated front-parallel trenches. Occurrence of bed rotation is particularly evident at the boundary between the claystone beds and the overlying sands. The collapsed portion was then subject to erosion, and gave rise to the formation of the dome-shaped forms. The different generations of dome-shaped forms show smaller dimensions and more symmetric profiles further away from the badland slopes, and are separated from each other by NW-SE trending trenches that sub-parallel the badlands slopes. Digital images permit to highlight the presence of inlet holes connected to pipe fluid conduits within the claystones, which localize in correspondence of the aforementioned fracture sets. This finding is similar to what it has been previously documented in carbonate and siliciclastic rocks (ie. Panza et al., 2016, 2019). The pipe fluid conduits emerge at the base of the dome-shaped forms.

We also note that most of the gullies occurring at the badland slopes were controlled by Set 2 fractures (Fig. 14). The formation of these gullies favoured the dissection of the badland slope over time, and therefore influenced the size, shape and geometry of the dome-shaped forms. It can be therefore concluded that the morphological aspects of the badland slopes and associated dome-shaped forms is strictly influenced by pre-existing structural elements such as dilation fractures and shear fractures in the studied claystones. In particular, Set 1b and Set 2 fractures profoundly affected the trenches and gullies, respectively. The former fracture set formed likely the loci for nucleation of the sliding surfaces solving the gravitational collapse of the badland slopes.

6.2. Pisticci study area

In the Pisticci area, S-dipping normal faults pertaining to Set 1b displace the previously formed Sets 2 and 3 fractures. Sets 2 fractures consist of joints and sheared joints that localize at the extensional

Fig. 8. Outcrop view and line drawing of the main structural elements documented at both Site #1 and Site #2, Aliano area. The stereograms report the true and restored attitude of great circles pertaining to the individual fracture sets. The number of measurements (N) is reported for each site.

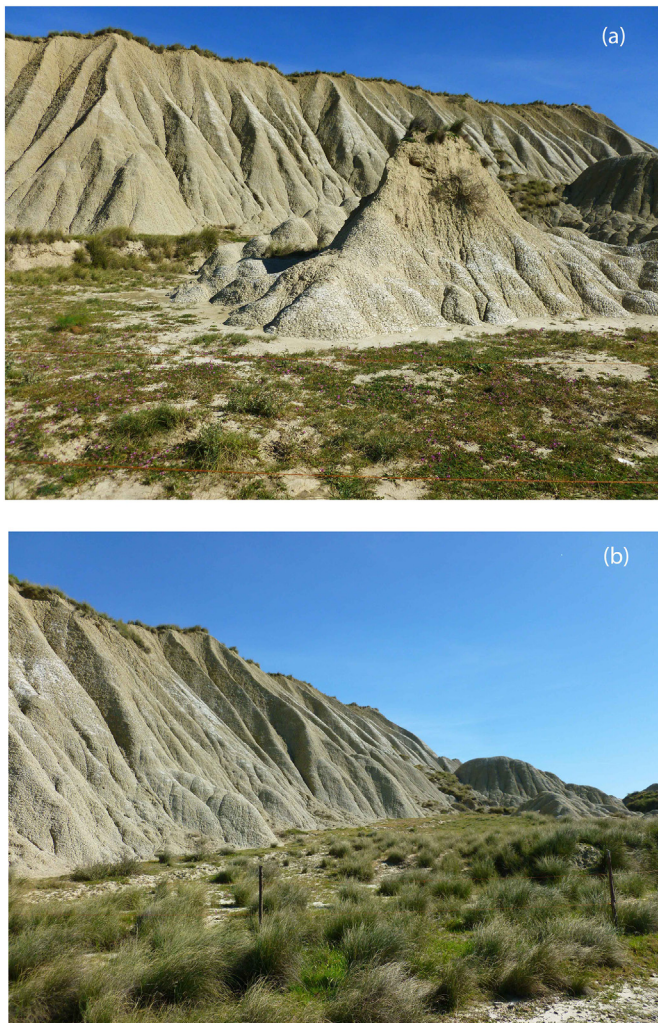


Fig. 10. Examples of badland slopes and associated dome-shaped forms from the Serra Pizzuta site (Pisticci area): a) Transect n.1 - badland slope and associated dome-shaped forms with colluvial deposits at the top; b) Transect n. 3- dome-shaped forms at the base of the badland slope.

quadrants of Set 3 fractures. The latter ones are N-S striking, left-lateral, strike-slip faults (cf. Fig. 11), which form the main tectonic lineaments of the study area. Occurrence of N-S striking, left-lateral, strike-slip faults in the area of the southern Bradano Trough was documented by Pieri et al. (1996) and Ciaranfi et al. (1979), and their activity is kinematically compatible with the present-day regional stress configuration of southern Italy (Montone et al., 2004) during transients of σ_1 and σ_2 permutation (Cello et al., 2003).

We documented that Set 2 (ca. NW-SE) and Set 3 (ca. N-S) fractures dissected the badlands' slope (Fig. 14). In addition, similar to the previous study area, Set 1 fractures (ca. E-W) favoured the gravitational collapse of the front and gave rise to formation of the dome-shaped forms, consistent with the mass movement and piping dominant stage proposed by Faulkner (2008). The inlet holes that localize in between the badland slope and the dome-shaped forms occur along Set 1 and Set 3 shear fractures. These inlet holes are connected to numerous pipe fluid conduits, which emerge at various heights along the flat areas located at the base of the badlands slope. All aforementioned structural elements are therefore consistent with the development of badlands

along an E-W direction by means of gravity-driven normal faults, which crosscut the claystones producing a cm-thick shear zone, characterized by both synthetic and antithetic Riedel-like sheared fractures (cf. Fig. 13).

6.3. Conceptual model of badland slopes and associated dome-shaped forms

The inferred control exerted by the aforementioned structural elements on the evolution of the badlands is summarized in the conceptual model below. The proposed model includes four main stages of activity, as shown in Figs. 15 and 16.

6.3.1. Stage I

At the beginning, a very steep badlands slopes (ca. 42°) originated through erosional processes connected to the general northward tilting and tectonic uplift of the area since the Middle Pleistocene, giving rise to a monoclinical systems with the steeper slopes exposed to the south (Joshi and Nagare, 2013; Mather et al., 2002; Piccarreta et al., 2006). The northward slope is controlled by the average dip angle of the claystone beds (ca. 12° N) and covered by vegetation. Small fissures sub-parallel to the badlands slope are present along the north-facing slope just above the scarp. These fissures localize along the laterally discontinuous Set 1b fractures.

6.3.2. Stage II

Subsequently, the aforementioned fissures become laterally continuous, and form small trenches affecting the upper portion of the north-facing badlands slope. These trenches are interrupted laterally by gullies either oblique (Aliano) or perpendicular (Pisticci) to the badland slopes due to pre-existing NW-SE striking (Set 2 fractures) or N-S striking (Set 3 fractures) discontinuities, respectively. During this stage, the badland slopes undergo a pronounced morphological evolution. The trench can be affected by a shear component, which produces a small displacement of the northern slope. Such a process is considered as causing the nucleation of the gravitational collapse, which will eventually involve the entire slope, re-activating Set 1b fractures. Due to the different dip angle of the claystone beds in the downthrown block, the gravitational collapse takes place by means of rotational sliding mechanisms.

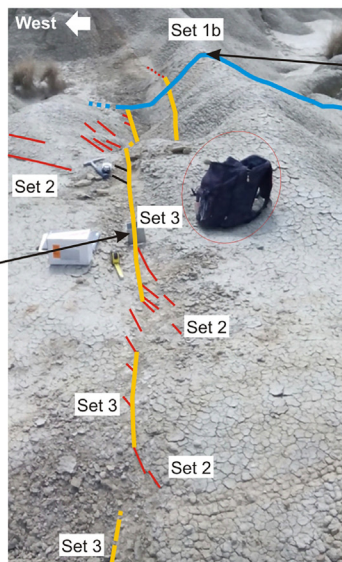
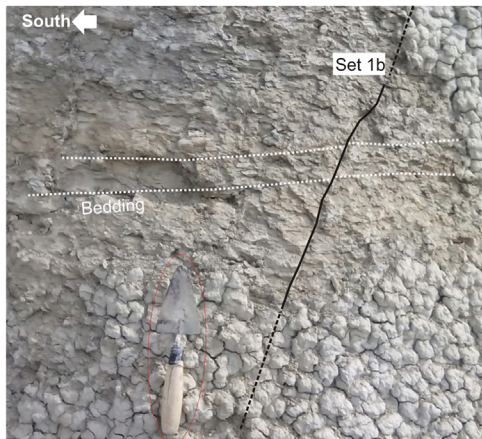
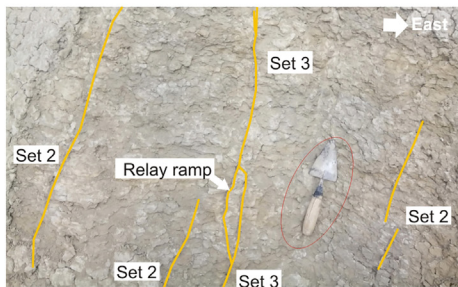
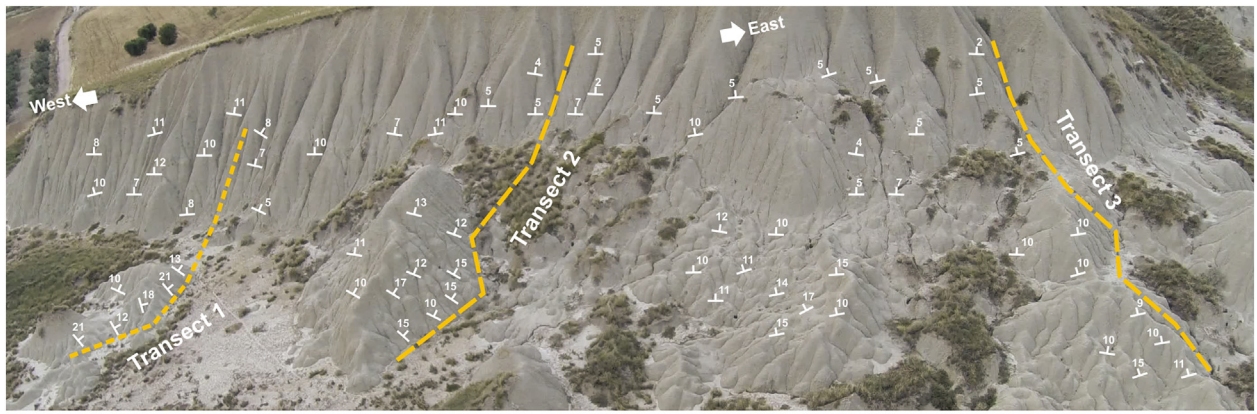
6.3.3. Stage III

The badland slopes are marked by several gullies that are sub-parallel to each other. Large, asymmetrical, dome-shaped forms develop at the base, close to the trench that separates them from the badland slope. The trench is due to deepening of the incipient trench predicted from the previous stage and localizes where the sliding surface intersects the badland slope. Ongoing gravitational collapse of the badlands causes the formation of dome-shaped forms. Later on, fragmentation of the claystones along the pre-existing Set 2 (Aliano) and Set 3 fractures (Pisticci) takes place. Erosional processes model the dome-shaped forms, producing their typical rounded appearance. Radial gullies develop, and colluvial deposits form at the base of both the badland slope and the dome-shaped forms (Piccarreta et al., 2006).

6.3.4. Stage IV

During the last evolutionary stage, the badlands slopes are crosscut by gullies whose orientation is conditioned by the pre-existing Set 2 fractures (Aliano) and Set 3 fractures (Pisticci). The streams are more incised than in the previous stage, and small debris flows and translational slides might develop along their sides affecting the uppermost, up to 1 m-thick altered portion of the claystone beds. Inlet holes, which convey

Fig. 11. Outcrop view and line drawing of the main structural elements documented along the three different transects performed at the Pisticci site. Bedding attitude of the claystone beds is reported in the topmost figure. Outcrop view of the main structural elements, and their relative abutting/crosscutting relations are shown in the figures at the centre. At the bottom, close ups of both Set 1a and Set 3 elements, of their sampled volumes, and of the abutting relations shown by Set 2 and Set 3 elements.



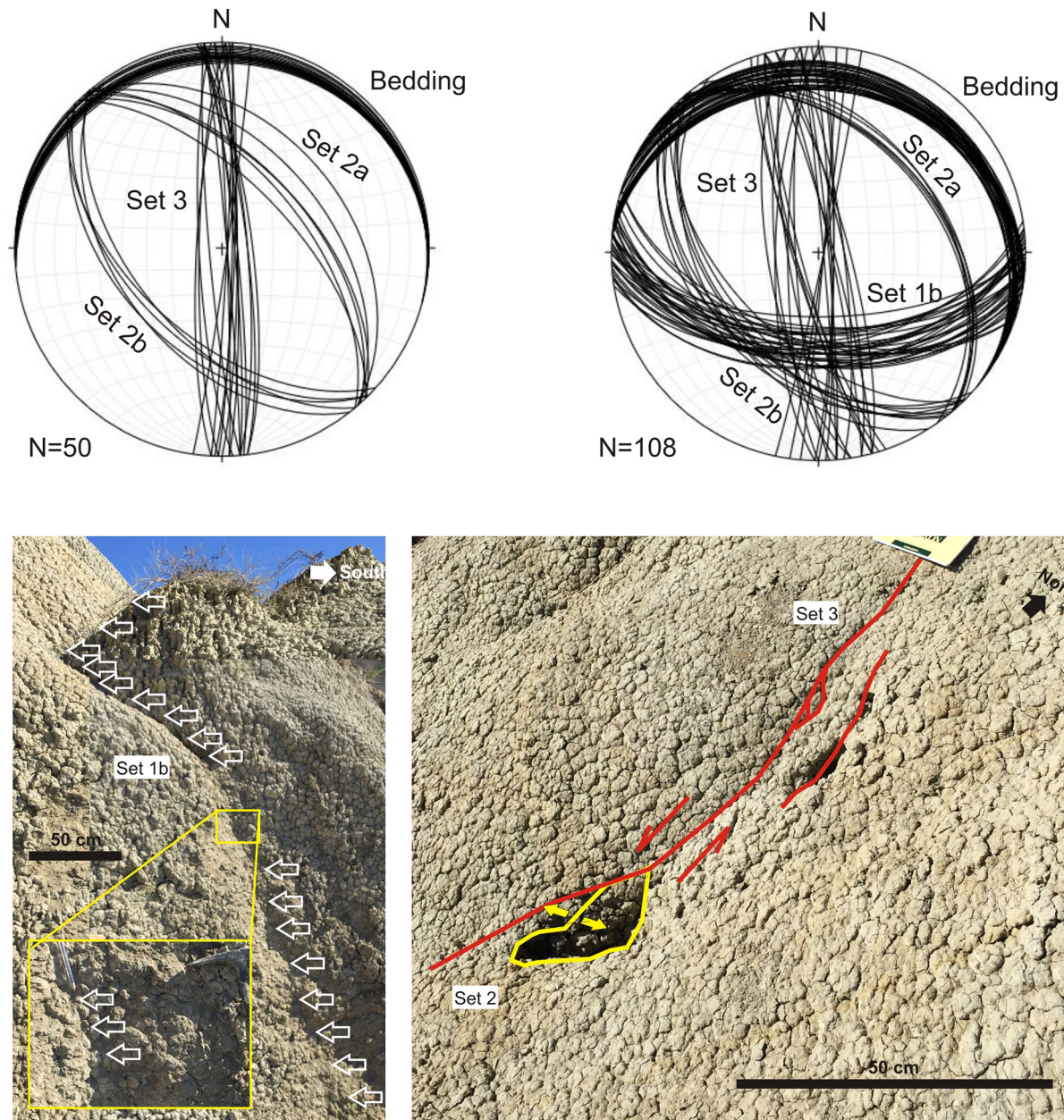


Fig. 12. Above, stereograms reporting the attitude (great circle) of the main structural elements documented at the badland slope and along the dome-shaped forms of the Pisticci site. The number of measurements (N) is reported. At the bottom, outcrop views of set 1B shear fractures, and of the abutting relations between Set 2 and Set 3 elements.

the water derived from the gullies incising the badland slopes, produce a network along the sliding surface.

Pipe fluid conduits hence form at the base of the slope, in correspondence with the trenches separating the badland slopes from the youngest dome-shaped forms. At Pisticci, the inlet holes localize at the intersection between Set 2 and Set 3 fractures. At Aliano, they localize at the intersection between Set 1b and Set 2 fractures. This outlines the importance of brittle discontinuity in promoting water circulation at shallow levels in clays.

6.4. Main factors influencing the development of the badland forms

The conceptual model proposed in this work improves earlier schemes introduced by previous authors (Piccarreta et al., 2006; Vergari et al., 2019) by providing evidence on the relationships between badlands evolution and discontinuities within the rock mass and by

explaining in more detail the origin of dome-shaped forms. The model can be applied to other areas where claystones underwent a comparable tectonic and geomorphological evolution, with the development of the badland slopes and associated dome-shaped forms (Vergari et al., 2019).

One of the key factors that controls the evolution of the badland forms is the outcropping lithology, which generally consists of clay with different percentages of silt (Moreno de las Heras and Gallart, 2018). Regarding the distribution of forms, some authors suggest that there are no substantial differences in particle sizes between samples taken on different badlands forms (Alexander, 1982; Piccarreta et al., 2006), while others indicate that the dome-shaped forms mainly affect silty clay (Battaglia et al., 2002; Sdao et al., 1984; Vittorini, 1977). Clays into which badlands develop are generally of marine origin and therefore rich in sodium, favoring a dispersive behaviour and the development of some forms including pipes (Faulkner, 2013; Piccarreta et al.,

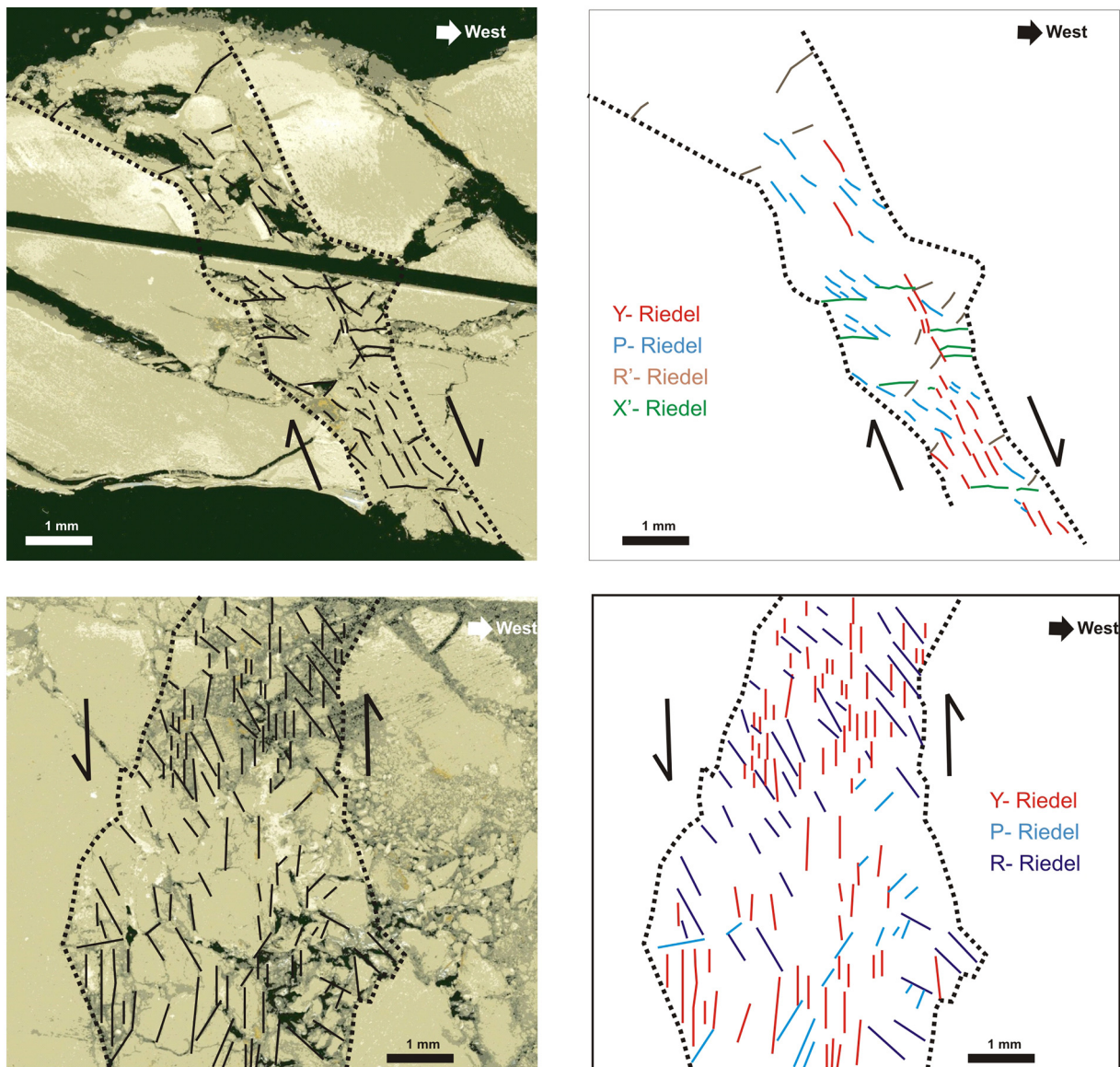


Fig. 13. Close ups (on the left) and line drawing (on the right) of the Riedel fractures documented within the samples collected along the Set 1a (bottom) and 3 (top) elements (cf. Fig. 14). See text for details.

2006; Vergari et al., 2013). The erosion rate due to atmospheric agents, mainly depends on the physical-chemical properties of the materials, on the development of macropores, on the climatic regimes and on the slope gradient (Schumm, 1956). The mineralogy of the surficial clays plays an important role on the evolution of the badland slopes because it influences the permeability of the material, the swelling capacity, the development of shrinkage cracks and the evolution of the slopes due to atmospheric agents.

The structural control on the development of different badland morphologies is provided primarily by the attitude of bedding planes in clays. In areas where clays are sub-horizontal, lowering of the base level induces an increase in the erosion and the formation of badlands only along slopes carved by the waterways. In this case less frequent but more prominent badland morphologies develop (Mather et al., 2002; Joshi and Nagare, 2013). In contrast, if dipping beds were generated by tectonic movements, badland morphologies are present in steeper slope developed up-dip with respect to the bedding planes (Piccarreta et al., 2006; Farifteh and Soeters, 2006), as observed in the studied badland forms.

Finally, our results indicate that the main factor responsible for the localization of both gravitational and erosional processes in badland slopes is represented by structural discontinuities within claystones. Moreover, fractures promote the localization of the piping process, which is considered one of the main causes of badlands erosion within Plio-Pleistocene clays and has an important role in the genesis of various badland forms (Piccarreta et al., 2006). In particular, the inlet holes of pipes, located along the trench separating the badland slope and the younger dome-shaped forms, form mainly at the intersection of different fractures sets.

7. Conclusions

The results of a multi-method study aimed at assessing the mechanisms of badlands formation and evolution in southern Italy, at the Aliano site of the Sant'Arcangelo Basin, and the Pisticci site of the Bradanic Trough, highlight the role played by pre-existing structural heterogeneities. Badlands were subjected over time to retrogressive gravitational processes, which affected Plio-Quaternary claystones that



Fig. 14. Panorama views acquired by Unmanned Aerial Vehicle (UAV) of the badland slopes and associated dome-shaped forms exposed in the Aliano (A) and Pisticci (B) sites, illustrating the morphological effects of NW-SE (Set 2) and N-S (Set 3) oriented fractures on the morphology of the studied badland fronts.

were subsequently modified by the erosive agents that generated groups of different dome-shaped forms. The structural elements formed in response to tectonic stress regimes, and were interpreted in light of their genetic nature, kinematics, attitude, geometry, relative timing of formation, and distribution throughout the studied sites.

Dilatant fractures, oriented ca. parallel to the badland slopes, determined a favorable condition for the nucleation of mass movements, whereas shear fractures oriented either oblique or perpendicular to the fronts conditioned both surface hydrography and location of the dome shaped forms. At the Aliano site, the dome-shaped forms were influenced by the NW-SE striking, strike-slip shear fractures. At the Pisticci site, their evolution was controlled by the pre-existing N-S striking shear fractures. The numerous inlet holes documented at both sites along the trenches separating the badland slopes from the dome-shaped forms localize at the intersections of high-angle fractures.

Results of this multi-method study were summarized in a four stages conceptual model. Each stage is characterized by specific mechanisms and includes representative sketches aimed at assessing the time-dependant evolution of the two studied sites. In the first two stages slope-parallel fissures reactivating previous tectonic discontinuities tend to enlarge and deepen due to erosion and the onset of gravitational processes. During stage III, initial development of dome-shaped forms is assisted by gravity-driven mass movements and erosion along pre-

existing shear fractures at high angles with respect to the badland slope. Further erosion and gravitational movements (stage IV), favoured by diffuse piping process, produces different generations of dome-shaped forms.

A profound link between structural and geomorphological processes was therefore proposed on the basis of the existing literature and interpreted original data. The proposed evolutionary model can be also applied to other areas where similar badland slopes are found and clayey lithologies underwent deformation, uplift and erosion in different tectonic settings.

Declaration of competing interest

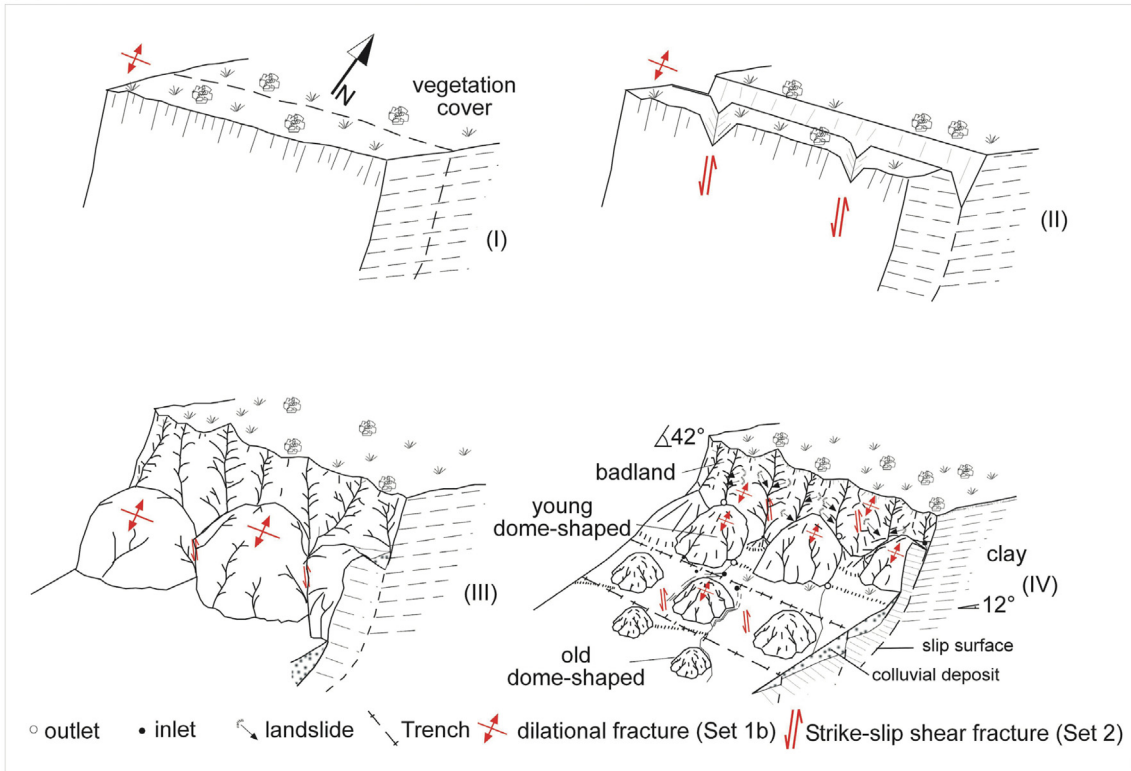
The authors declare that they have no known competing financial interests or personal relationships that could have appeared to influence the work reported in this paper.

Acknowledgments

We are very grateful to M. Stokes, H. Faulkner and two anonymous reviewers for the constructive comments to the manuscript. The authors also acknowledge the contribution provided by Michele Tricarico

Fig. 15. Conceptual model envisioned for the formation and evolution of badland slopes and associated dome-shaped forms in the studied area of Aliano. The accompanying pictures portray geomorphological settings related to specific evolutionary stages proposed for both areas.

(A)



(B)



Stage I



Stage II



Stage III



Stage IV

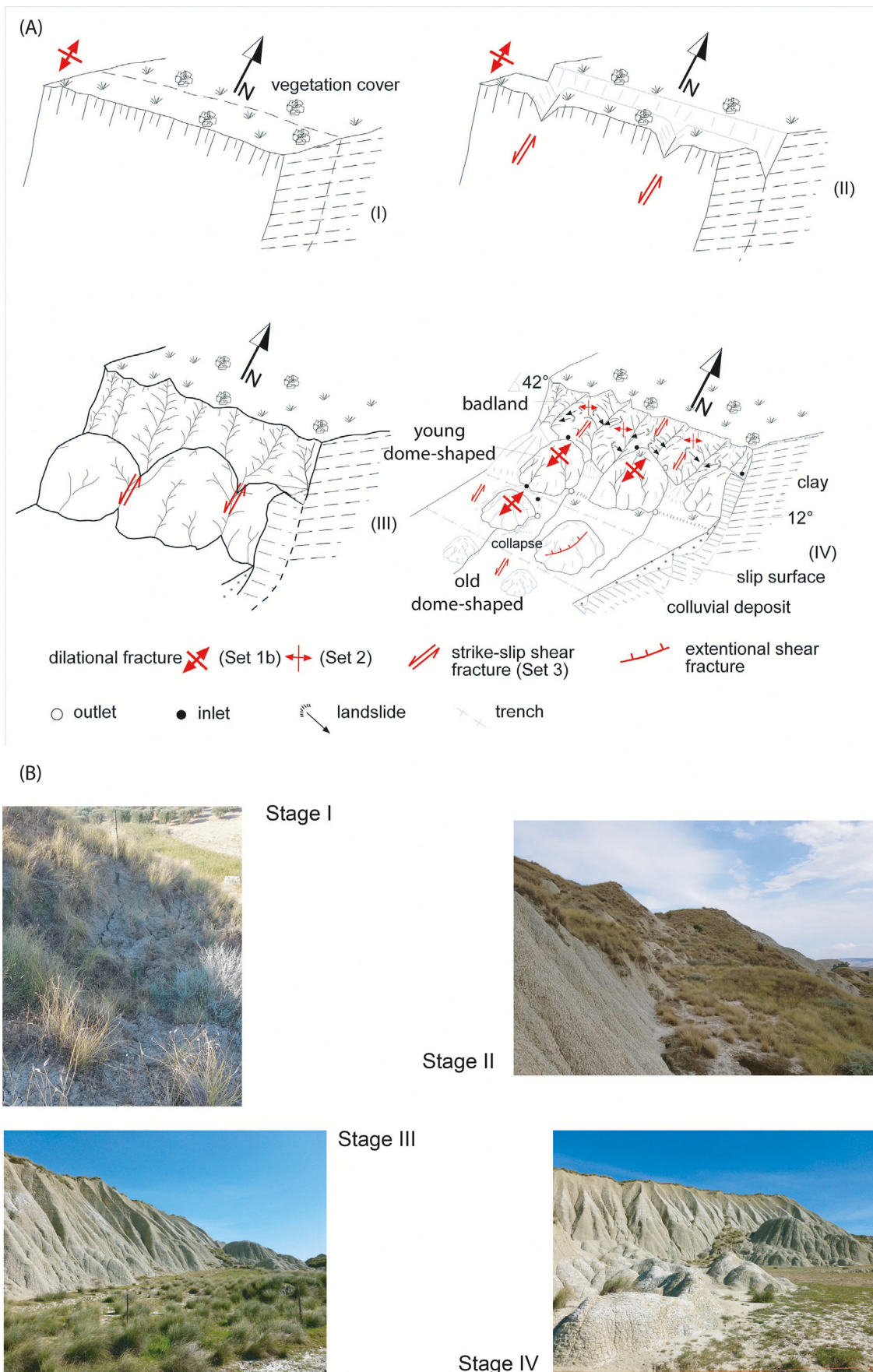


Fig. 16. Conceptual model envisioned for the formation and evolution of badland slopes and associated dome-shaped forms in the studied area of Pisticci. The accompanying pictures portray geomorphological settings related to specific evolutionary stages proposed for both areas.

and Domenico Sisto during both field and laboratory work. The present work was funded by RIL 2006 grants appointed to M. Bentivenga and F. Agosta.

References

- Agosta, F., Aydin, A., 2006. Architecture and deformation mechanism of a basin-bounding normal fault in Mesozoic platform carbonates, central Italy. *J. Struct. Geol.* 28, 1445–1467.
- Alexander, D.E., 1982. Difference between “calanchi” and “biancane” badlands in Italy. In: Bryan, R.B., Yair, A. (Eds.), *Badland Geomorphology and Piping*. Geobooks, Norwich, UK, pp. 71–87.
- Amato, A., 2000. Estimating Pleistocene tectonic uplift rates in the South-eastern Apennines (Italy) from erosional land surfaces and marine terraces. In: Slaymaker, O. (Ed.), *Geomorphology, Human Activity and Global Environmental Change*. Wiley, Chichester, pp. 67–87.
- Balduzzi, A., Casnedi, R., Crescenti, U., Tonna, M., 1982. Il Plio-Pleistocene del sottosuolo del bacino lucano (Avanfossa Appenninica). *Geol. Romana* 21, 89–111.
- Battaglia, S., Leoni, L., Sartori, F., 2002. Mineralogical and grain size composition of clays developing calanchi and biancane erosional landforms. *Geomorphology* 49, 153–170.
- Bavusi, M., Chianese, D., Giano, S.I., Mucciarelli, M., 2004. Multidisciplinary investigations on the Grumentum Roman aqueduct (Basilicata, southern Italy). *Ann. Geophys.* 47, 1791–1801.
- Bentivenga, M., Piccarreta, M., 2016. Geomorphological map of Pisticci area (Basilicata, Southern Italy). *J. Maps* <https://doi.org/10.1080/17445647.2016.1193776>.
- Bentivenga, M., Coltorti, M., Prosser, G., Tavarnelli, E., 2004a. Recent extensional faulting in the Gulf of Taranto area: implications for nuclear waste storage in the vicinity of Scanzano Ionico (Basilicata). *Boll. Soc. Geol. It.* 123, 391–404.
- Bentivenga, M., Coltorti, M., Prosser, G., Tavarnelli, E., 2004b. A new interpretation of terraces in the Taranto Gulf: the role of extensional faulting. *Geomorphology* 60, 383–402.
- Bentivenga, M., Foresi, L.M., Prestera, A., Prosser, G., Sabia, M., 2005. Structures located at the front of a thrust and fold belt: the Craco area (Southern Apennines, Italy). *Boll. Soc. Geol. It.* 124 (2), 367–376.
- Bentivenga, M., Capolongo, D., Palladino, G., Piccarreta, M., 2015. Geomorphological map of the area between Craco and Pisticci (Basilicata, Italy). *J. Maps* 11, 2015. <https://doi.org/10.1080/17445647.2014.935501>.
- Calamita, F., Coltorti, M., Pieruccini, P., Pizzi, A., 1999. Evoluzione strutturale e morfogenesi plio-quaternaria dell'Appennino umbro-marchigiano tra il preappennino umbro e la costa adriatica. *Boll. Soc. Geol. It.* 118, 125–139 (6 sheets).
- Caldara, M., Loiacono, F., Morlotti, E., Pieri, P., Sabato, L., 1988. Caratteri geologici e paleoambientali dei depositi plio-pleistocenici del bacino di S. Arcangelo (parte settentrionale): Italia meridionale. *Atti del 74° Congr. Naz. Soc. Geol. It.*: 'L'Appennino campano-lucano nel quadro geologico dell'Italia meridionale', Sorrento, 13–17 September 1988, pp. 51–58.
- Calzolari, C., Ungaro, F., 1998. Geomorphic features of a badland (biancane) area (Central Italy): characterisation, distribution and quantitative spatial analysis. *Catena* 31, 237–256.
- Caputo, R., Salviuolo, L., Bianca, M., 2007. Late Quaternary activity of the Scorciabuoi Fault (southern Italy) as inferred from morphotectonic investigations and numerical modeling. *Tectonics* 27 (TC 3004).
- Casciello, E., 2002. Deformazioni da taglio in materiali argillosi: Analisi dei sedimenti deformati dalla faglia di Scorciabuoi. *Studi Geol. Camerti* 1, 51–62.
- Casciello, E., Cesarano, M., Ferranti, M., Oldow, J.S., Pappone, G., 2000. Pleistocene noncoaxial fold development in the northern portion of the S. Arcangelo basin (Southern Apennines). *Mem. Soc. Geol. Ital.* 55, 133–140.
- Casnedi, R., 1988. La Fossa Bradanica: Origini, Sedimentazione e Migrazione. *Mem. Soc. Geol. It.* 41, 439–448 (7 sheets).
- Castaldi, F., Chiochini, U., 2012. Effects of landuse changes on badland erosion in clayey drainage basin radicefani, central Italy. *Geomorphology* 169 (170), 98–108.
- Catalano, S., Monaco, C., Tortorici, L., Tansi, C., 1993. Pleistocene strike-slip tectonics in the Lucanian Apennine (southern Italy). *Tectonics* 12 (3), 656–665. <https://doi.org/10.1029/92TC02251>.
- Cello, G., Tondi, E., Micarelli, L., Mattioni, L., 2003. Active tectonics and earthquake sources in the epicentral area of the 1857 Basilicata earthquake (southern Italy). *J. Geodyn.* 36, 37–50.
- Ciaranfi, N., Maggiore, M., Pieri, P., Rapisardi, L., Ricchetti, G., Walsh, N., 1979. Considerazioni sulla neotettonica della Fossa Bradanica. Contributi preliminari alla realizzazione della Carta Neotettonica d'Italia. *Prog. Fin. Geodinamica* 251, pp. 73–95.
- Cinque, A., Patacca, E., Scandone, P., Tozzi, M., 1993. Quaternary kinematic evolution of the Southern Apennines. Relationships between surface geological features and deep lithospheric structures. *Ann. Geofis.* 46, 249–260.
- Colica, A., Guasparri, G., 1990. Sistemi di fratturazione nelle argille plioceniche del territorio senese. Implicazioni geomorfologiche. *Atti dell'Accademia di Fisiocritici in Siena*. vol. 9 pp. 29–36.
- Cotecchia, V., Magri, G., 1967. Gli spostamenti della linea di costa quaternaria del mar Ionico tra Capo Spulico e Taranto. *Geol. Appl. Idrogeol.* 2, 1–27.
- D'Argenio, B., Alvarez, W., 1980. Stratigraphic evidence for crustal thickness changes on the southern Tethyan margin during the Alpine cycle. *Geol. Soc. Am. Bull.* 91, 681–689.
- D'Argenio, B., Pescatore, T., Scandone, P., 1973. Schema geologico dell'Appennino Meridionale. *Atti del convegno “Moderne vedute sulla geologia dell'Appennino”*. Accad. Nazionale Lincei, Quaderno 183, 49–72.
- Del Monte, M., 2017. The typical badlands landscapes between the Tyrrhenian Sea and the Tiber River. *Landscape and Landforms of Italy* 281–291.
- Del Prete, M., Bentivenga, M., Coppola, L., Rendell, H., 1994. Aspetti evolutivi dei reticoli calanchivi a Sud di Pisticci (MT). *Geol. Romana* 30, 295–306.
- Del Prete, M., Bentivenga, M., Amato, M., Basso, F., Tacconi, P., 1997. Blandland erosion processes and their interactions whit vegetation: a case study from Pisticci, Basilicata, Southern Italy. *Geogr. Fis. Din. Quat.* 20 (147–155), 15.
- Dogliani, C., 1991. Una interpretazione della tettonica globale. *Le Scienze* 270, 32–42.
- Dramis, F., Gentili, B., Coltorti, M., Cherubini, C., 1982. Osservazioni geomorfologiche sui calanchi marchigiani. *Geogr. Fis. Din. Quat.* 5, 38–45.
- Farifteh, J., Soeters, R., 1999. Factors underlying piping in the Basilicata region, southern Italy. *Geomorphology* 26, 239–251.
- Farifteh, J., Soeters, R., 2006. Origin of biancane and calanchi in East Aliano, southern Italy. *Geomorphology* 77, 142–152.
- Faulkner, H., 2008. Connectivity as a crucial determinant of badland morphology and evolution. *Geomorphology* 100, 91–103. <https://doi.org/10.1016/j.geomorph.2007.04.039>.
- Faulkner, H., 2013. Badlands in mail lithology: a field guide to soil dispersion, subsurface erosion and piping-origin gullies. *Catena* 106, 42–53.
- Ghisetti, F., Vezzani, L., 1999. Depth and modes of Pliocene–Pleistocene crustal extension of the Apennines (Italy). *Terra Nova* 11, 67–72.
- Ghisetti, F., Kirschner, D.L., Vezzani, L., Agosta, F., 2001. Stable isotope evidence for contrasting paleofluid circulation in thrust faults and normal faults of the central Apennines, Italy. *J. Geophys. Res.* 106, 8811–8825.
- Giano, S.I., Giannandrea, P., 2014. Late Pleistocene differential uplift inferred from the analysis of fluvial terraces (southern Apennines, Italy). *Geomorphology* 217, 89–105.
- Giano, S.I., Pescatore, E., Agosta, F., Prosser, G., 2018. Geomorphic evidences of Quaternary tectonics in an underlap fault zone of southern Apennines, Italy. *Geomorphology* 303, 172–190.
- Hearthly, P., Dai Pra, G., 1992. The age and stratigraphy of Middle Pleistocene and younger deposits along the Gulf of Taranto (Southeast Italy). *J. Coast. Res.* 8, 882–905.
- Hippolyte, J.C., Angelier, J., Roure, F., Müller, C., 1991. Géométrie et mécanisme de formation d'un bassin “piggyback”: le bassin de Sant'Arcangelo (Italie méridionale). *CR Acad. Sci. Paris* 312, 1373–1378.
- Hippolyte, J.C., Angeliere, J., Roure, F., Casero, P., 1994. Piggyback basin development and thrust belt evolution: structural and palaeostress analyses of Plio-Quaternary basins in the Southern Apennines. *J. Struct. Geol.* 16, 159–173.
- Joshi, V.U., Nagare, V.B., 2013. Badland formation along the Pravara River, Western Decan, India. Can neotectonics be the cause? *Z. Geomorphol.* 57, 349–370. <https://doi.org/10.1127/0372-8854/2013/0109>.
- La Bruna, V., Agosta, F., Prosser, G., 2017. New insights on the structural setting of the Monte Alpi area, Basilicata, Italy. *Ital. J. Geosci.* 132, 220–237.
- La Bruna, V., Agosta, F., Lamarche, J., Viseur, S., Prosser, G., 2018. Fault growth mechanisms and scaling properties in foreland basin system: the case study of Monte Alpi, Southern Apennines, Italy. *J. Struct. Geol.* 116, 94–113.
- Lentini, F., Vezzani, L., 1974. Note illustrative del Foglio 506 S. Arcangelo. I.R.P.I. p. 46.
- Mantovani, E., Albarello, D., Tamburelli, C., Babbucci, D., 1996. Evolution of the Tyrrhenian basin and surrounding regions as result of the Africa-Eurasia convergence. *J. Geodyn.* 21, 35–72.
- Mather, A.E., Stokes, M., Griffiths, J.S., 2002. Quaternary landscape evolution: a framework for understanding contemporary erosion, southeast Spain. *Land Degrad. Dev.* 13, 89–109. <https://doi.org/10.1002/ldr.484>.
- Mazzoli, S., Aldega, L., Corrado, S., Invernizzi, C., Zattin, M., 2006. Pliocene-Quaternary thrusting, syn-orogenic extension and tectonic exhumation in the Southern Apennines (Italy): insights from the Monte Alpi area. *Geol. Soc. Am. Spec. Pap.* 414, 55–77.
- Menardi Noguera, A., Rea, G., 2000. Deep structure of the Campanian-LucanianArc (Southern Apennine, Italy). *Tectonophysics* 324, 239–265.
- Migliorini, C., 1937. Cenno sullo studio e sulla prospezione petrolifera di una zona dell'Italia meridionale. 2nd Petro-leumworld Congress, Paris, AGIP Report, pp. 1–11.
- Monaco, C., Tortorici, L., Paltrinieri, W., 1998. Structural evolution of the Lucanian Apennines, southern Italy. *J. Struct. Geol.* 20, 617–638.
- Montone, P., Mariucci, M.T., Pondrelli, S., Amato, A., 2004. An improved stress map for Italy and surrounding regions (Central Mediterranean). *J. Geophys. Res.* 109, B10410. <https://doi.org/10.1029/2003JB002703>.
- Moreno de las Heras, M., Gallart, F., 2018. The origin of Badlands. In: Nadal-Romero, Estela, Martínez-Murillo, Juan F., Kuhn, Nikolaus J. (Eds.), *Badlands Dynamics in a Context of Global Change*, pp. 27–59.
- Moretti, S., Rodolfi, G., 2000. A typical “calanchi” landscape on the Eastern Apennine margin Atri, Central Italy geomorphological features and evolution. *Catena* 40, 217–228.
- Myers, R., Aydin, A., 2004. The evolution of faults formed by shearing across joint zones in sandstone. *J. Struct. Geol.* 26, 947–966.
- Neboit, R., 1982. Instabilité et morphogenèse au Quaternaire en Lucania orientale. *Revue de Géographie Physique et de Géologie dynamique*. vol. 23, pp. 15–26.
- Neugir, F., Stark, M., Kaiser, A., Vlacilova, M., Della Seta, M., Vergari, F., Schmidt, J., Becht, M., Haas, F., 2016. Erosion processes in calanchi in the Upper Orcia Valley, Southern Tuscany, Italy based on multitemporal high-resolution terrestrial LiDAR and UAV surveys. *Geomorphology* 269, 8–22. <https://doi.org/10.1016/j.geomorph.2016.06.027>.
- Ogniben, L., 1969. Schema introduttivo alla geologia del confine calabro-lucano. *Memorie della Società Geologica Italiana*, VIII, 4, Pisa.
- Palladino, G., 2011. Tectonic and eustatic controls on Pliocene accommodation space along the front of the southern (Basilicata, southern Italy). *Basin Res.* 23, 591–614. <https://doi.org/10.1111/j.1365-2117.2011.00503.x>.
- Panza, E., Agosta, F., Rustichelli, A., Zambrano, M., Tondi, E., Prosser, G., Giorgioni, M., Janiseck, J.M., 2016. Fracture stratigraphy and fluid flow properties of shallow water, tight carbonates: the case study of the Murge Plateau (southern Italy). *Mar. Pet. Geol.* 73, 350–370.
- Panza, E., Agosta, F., Rustichelli, A., Vinciguerra, S., Ougier-Simonin, A., Dobbs, M.R., Prosser, G., 2019. Meso-to-microscale fracture porosity in tight limestones, results of an integrated field and laboratory study. *Mar. Pet. Geol.* 103, 581–595.

- Patacca, E., Scandone, P., 2001. Late thrust propagation and sedimentary response in the thrust-belt-foredeep system of the South-ern Apennines (Pliocene-Pleistocene). In: VAI, G.B., Martini, I.P. (Eds.), *Anatomy of an Orogen: The Apennines and the Adja-Cent Mediterranean Basins*. Kluwer Academic Publishers, Dordrecht, The Netherlands, pp. 401–440.
- Patacca, E., Scandone, P., 2007. Geology of the Southern Apennines. *Boll. Soc. Geol. It. Ital. J. Geosci.* 7, 75–119.
- Piccarreta, M., Capolongo, D., Bentivenga, M., Pennetta, L., 2005. Precipitation and Dry-Wet Cycles Influence on Badland Development in a Semi-arid Area of Basilicata Region (Southern Italy) *Geografia Fisica e Dinamica Quaternaria*, VII, pp. 281–289.
- Piccarreta, M., Faulkner, H., Bentivenga, M., Capolongo, D., 2006. The influence of physico-chemical material properties on erosion processes in the badlands of Basilicata, Southern Italy. *Geomorphology* 81, 235–251.
- Piccarreta, M., Pasini, A., Capolongo, D., Lazzari, M., 2013. Changes in daily precipitation extremes in the Mediterranean from 1951 to 2010: the Basilicata region, southern Italy. *Int. J. Climatol.* 33, 3229–3248. <https://doi.org/10.1002/joc.3670>.
- Piccarreta, M., Lazzari, M., Pasini, A., 2015. Trends in daily temperature extremes over the Basilicata Region (southern Italy) from 1951 to 2010 in a Mediterranean climatic context. *Int. J. Climatol.* 35 (8), 1964–1975.
- Pieri, P., Sabato, L., Loiacono, F., Marino, M., 1994. Il bacino piggyback di Sant'Arcangelo: evoluzione tettonico-sedimentaria. *Boll. Soc. Geol. It.* 113, 465–481.
- Pieri, P., Sabato, L., Tropeano, M., 1996. Significato geodinamico dei caratteri deposizionali e strutturali della Fossa Bradanica nel Pleistocene. *Mem. Soc. Geol. It.* 51, 501–515.
- Pieri, P., Vitale, G., Beneduce, P., Doglioni, C., Gallicchio, S., Giano, S.I., Loizzo, R., Moretti, M., Prosser, G., Sabato, L., Schiattarella, M., Tramutoli, M., Tropeano, M., 1997. Tettonica quaternaria dell'area bradanico-ionica. *Il Quaternario* 10, 535–542.
- Roure, F., Casero, P., Vially, R., 1991. Growth processes and mélange formation in the southern Apennines accretionary wedge. *Earth Planet. Sci. Lett.* 102, 395–412.
- Royden, L.H., Patacca, E., Scandone, P., 1987. Segmentation and configuration of subducted lithosphere in Italy: an important control on thrust-belt and foredeep-basin evolution. *Geology* 15, 714–717.
- Sabato, L., 1997. Sedimentary and tectonic evolution of a lower-middle Pleistocene lacustrine system in the Sant'Arcangelo piggyback basin (southern Italy). *Geol. Romana* 33 (1), 137–145.
- Schiattarella, M., Di Leo, P., Beneduce, P., Giano, S.I., Martino, C., 2006. Tectonically driven exhumation of a young orogen: an example from the southern Apennines, Italy. In: Willett, S.D., Hovius, N., Brandon, M.T., Fisher, D.M. (Eds.), *Tectonics, Climate, and Landscape Evolution*, Geological Society of America Special Paper 398, Penrose Conference Series, pp. 371–385.
- Schiattarella, M., Giano, S.I., Gioia, D., Martino, C., Nico, G., 2013. Age and statistical properties of the summit palaeosurface of southern Italy. *Geogr. Fis. Din. Quat.* 289–302. https://doi.org/10.4461/GFDQ.2013.36.23_36 (2013).
- Scholz, C.H., 2002. *The Mechanics of Earthquakes and Faulting*. Cambridge University Press, New York, p. 519.
- Schumm, S.A., 1956. The role of creep and rainwash on the retreat of badland slopes. *Am. J. Sci.* 254, 693–705.
- Sdao, G., Simone, A., Vittorini, S., 1984. Osservazioni geomorfologiche su calanchi e biancane in Calabria. *Geografia Fisica e Dinamica del Quaternario* 7, 10–16.
- Selli, R., 1962. Il Paleogene nel quadro della geologia dell'Italia meridionale. *Mem. Soc. Geol. Ital.* 3, 737–790.
- Shiner, P., Beccacini, A., Mazzoli, S., 2004. Thin-skinned versus thick-skinned structural models for Apulian Carbonate Reservoirs: constraints from the Val D'Agri Field. *Mar. Pet. Geol.* 21, 805–827.
- Summa, V., Tateo, F., Medici, F., Giannosi, M.L., 2007. The role of mineralogy, geochemistry and grain size in badland development in Pisticci (Basilicata, Southern Italy). *Earth Surf. Process. Landf.* 32, 980–997.
- Torri, D., Bryan, R., 1997. Micropiping processes and biancana evolution in southeast Tuscany, Italy. *Geomorphology* 20, 219–235.
- Torri, D., Colica, A., Rockwell, D., 1994. Preliminary study of the erosion mechanisms in biancane badland (Tuscany, Italy). *Catena* 23, 281–294.
- Turco, E., Maresca, R., Cappadona, P., 1990. La tettonica plio-pleistocenica del confine calabro-lucano: modello cinematico (Plio-Pleistocene tectonics at the Calabrian-Lucanian boundary: a kinematic model). *Mem. Soc. Geol. Ital.* 45, 519–529.
- Twiss, R.J., Moores, E.M., 2007. *Structural Geology*. W.H. Freeman and Company, New York, p. 736.
- Vergari, F., Della Seta, M., Del Monte, M., Fredi, P., Palmieri, E.L., 2011. Landslide susceptibility assessment in the Upper Orcia Valley (Southern Tuscany, Italy) through conditional analysis: a contribution to the unbiased selection of causal factors. *Nat. Hazards Earth Syst. Sci.* 11 (5), 1475.
- Vergari, F., Della Seta, M., Del Monte, M., Barbieri, M., 2013. Badlands denudation 'hot spots': the role of parent material properties on geomorphic processes in 20-years monitored sites of Southern Tuscany (Italy). *Catena* 106, 31–41. <https://doi.org/10.1016/j.catena.2013.06.016>.
- Vergari, F., Troiani, F., Faulkner, H., Del Monte, M., Della Seta, M., Ciccacci, S., Fredi, P., 2019. The use of the slope–area function to analyse process domains in complex badland landscapes. *Earth Surf. Process. Landf.* 44, 273–286. <https://doi.org/10.1002/esp.4496>.
- Vezzani, L., 1967. Il bacino plio-pleistocenico di S. Arcangelo (Lucania). *Atti Acc. Gioenia Sc. Nat. Catania* 18, 207–227.
- Vezzani, L., Festa, V., Ghisetti, F., 2010. Geology and tectonic evolution of the Central-Southern Apennines, Italy. *Geol. Soc. Am. Spec. Pap.* 469, 1–58.
- Vittorini, S., 1977. Osservazioni sull'origine e sul ruolo di due forme di erosione nelle argille: calanchi e biancane – *Bollettino della Società Geografica Italiana*, serie X, vol. VI, pp. 25–54.
- Westaway, R., 1993. Quaternary Uplift of Southern Italy. *J. Geophys. Res.* 98, 741–772.
- Westaway, R., Bridgland, D., 2007. Late Cenozoic uplift of southern Italy deduced from fluvial and marine sediments: coupling between surface processes and lowercrustal flow. *Quat. Int.* 175, 86–124.
- Zavala, C., Mutti, E., 1996. Stratigraphy of the Plio-Pleistocene Sant'Arcangelo Basin, Southern Apennines, Basilicata, Italy. *Atti Gruppo Informale di Sedimentologia, Catania*, pp. 279–282.